energies

MDPI

Article

Coupled Model of Heat and Mass Balance for Droplet Growth in Wet Steam Non-Equilibrium Homogeneous Condensation Flow

Xu Han [1], Zhonghe Han [1,*], Wei Zeng [1], Jiangbo Qian [1,2] and Zhi Wang [1]

[1] Key Lab of Condition Monitoring and Control for Power Plant Equipment, North China Electric Power University, Ministry of Education, Baoding 071003, China; xuhan@ncepu.edu.cn (X.H.); 1142102033@ncepu.edu.cn (W.Z.); 51451329@ncepu.edu.cn (J.Q.); wangzhi@ncepu.edu.cn (Z.W.)

[2] Research Institute of BIT in Zhongshan, Zhongshan 528400, China

* Correspondence: hanzhonghe@ncepu.edu.cn; Tel.: +86-312-752-2100

Received: 17 November 2017; Accepted: 29 November 2017; Published: 2 December 2017

Abstract: Because of the complexity of wet steam two-phase condensation flow, many problems remain to be solved. The important part of condensation theory—the calculation of the water droplet growth model in the transition zone—is not ideal; thus, it is necessary to develop a water droplet growth model with full-scale range. On the basis of the heat and mass transfer equilibrium in droplet growth, a coupled model of heat and mass balance for droplet growth is proposed. To verify the accuracy of this model, the differences and applicable ranges of various models were analysed using the experimental data of Peters and Meyer and two widely used models. In the free molecular flow region, the heat and mass balance model coincides with the Young low-pressure correction model. In the transition region, the heat and mass balance model agrees well with the experimental values of Peters and Meyer. In the continuous flow region, the heat and mass balance model coincides with the Gyarmathy model. Therefore, the heat and mass balance model can be used to accurately describe the growth process of water droplets in the arbitrary range of Knudsen numbers.

Keywords: wet steam; Knudsen number; water droplet growth model; two-phase flow; condensation; thermodynamics

1. Introduction

The development level of the electric power industry is an important index for measuring the modernisation degree of a country. The steam turbine, as a type of power generator, plays an important role in the safe and economical operation of power plants [1]. The statistics of thermal power and nuclear power generation in China from 2010 to 2016 are shown in Table 1. In 2016, thermal power and nuclear power generation capacity accounted for approximately 78% of China's power generation capacity. Given China's energy structure, power generation in the next few decades will continue to rely on steam turbines.

Spontaneous two-phase condensation flow in a steam turbine is very complex and involves many disciplines of computational fluid dynamics, multiphase flow, heat and mass transfer, statistical thermodynamics, and gas dynamics. Existing research on wet steam condensation flow can be divided into four approaches: condensation theory, experimental research, numerical research, and analytical research [2,3]. The wet steam spontaneous condensation and droplet growth process occurs at the nanometre scale, and micro-droplet surface tension and mass transfer have always been difficult problems. Condensation theory includes the nucleation model and the water droplet growth model [4]. However, the calculation of non-equilibrium condensation flow involves many

uncertainties. By comparing a large volume of experimental data, Han et al. found a certain deviation between the predictions of classical nucleation theory and experimental values; they also observed that the calculation of the existing water droplet growth model in the transition zone is not ideal [5].

Table 1. Thermal power and nuclear power generation in China.

Year	Total Power Generation/ 10^8 kW·h	Thermal Power Generation/ 10^8 kW·h	Nuclear Power Generation/ 10^8 kW·h
2010	42,280	34,145 (80.76%)	768 (1.82%)
2011	47,217	38,975 (82.54%)	874 (1.85%)
2012	49,774	39,108 (78.60%)	982 (1.97%)
2013	53,474	41,900 (78.36%)	1121 (2.10%)
2014	56,801	43,030 (75.76%)	1332 (2.35%)
2015	57,399	42,307 (73.71%)	1714 (2.99%)
2016	59,111	43,958 (74.37%)	2127 (3.60%)

The droplets in the initial growth stage are located in the molecular free flow region. The water molecules in the steam collide with water droplets and then merge with them; the growth mechanism of water droplets can be described by a molecular dynamics model. However, when the droplet radius is far greater than the vapour mean free path, droplets will be in a continuous flow region and the droplet growth mechanism can be described by the kinetic model of the continuum hypothesis. Most of the water droplets in the low-pressure cylinder of the turbine are 1–500 nm, belonging to the free flow region and the transition zone. Therefore, choosing an appropriate water droplet growth model is the key to accurately calculating wet steam condensation flow.

On the basis of the Fick diffusion theorem and the Fourier thermal conductivity calculation equation, Gyarmathy determined the relationship of the heat transfer coefficient of a water droplet and established the water droplet growth model [6]. The Gyarmathy model is accurate in the continuous flow region and the molecular free flow region; however, the calculated values in the transition region have some errors. On the basis of the energy balance model and molecular dynamics theory, Hill calculated the water droplet growth rate [7]; however, because Hill's equation is more complex and the results are basically consistent with the Gyarmathy model, its application is not widespread. Young's group developed a low-pressure modified droplet growth model by assuming that a transition layer exists between water droplets and the surrounding steam [8,9]. The flow relationship between a water droplet and the transition layer and that between the transition layer and steam are determined using the Langmuir three-layer theoretical model. Heiler [10] used the Fuchs–Sutugin difference formula to correct the correction factor of the Gyarmathy model. Delale and Meier [11] took the growth model of the molecular free flow region and continuous flow region into the transition region and obtained the water droplet growth model for the transition zone from the numerical solution. Bakhtar et al. [12,13] speculated that, when the droplet diameter is far greater than the vapour molecular mean free path, the vapour migration velocity and liquid vapour pressure difference between the two phases can be neglected. On the basis of this hypothesis, a water droplet growth model in the continuous flow region was proposed. The Gyarmathy model and the Young low-pressure correction model are well used to calculate the water droplet growth rate, with the Young model being the most widely used. In general, the theory of water droplet growth has developed rapidly and the basic work has been improved; however, some remaining problems need to be solved. Most of the condensation flow in a steam turbine is located in the low-pressure transition zone; however, few models can accurately calculate the growth process of the full size range of droplets.

2. Water Droplet Growth Model

2.1. Droplet Growth Theory

Because the nucleation time is very short, the wet steam is in the water droplet growth region after the nucleation process until the cascade exit. The whole process of water droplet growth is

accompanied by heat and mass transfer phenomena. Steam molecules on the surface of the water condense and release latent heat. The critical water droplet radius is 10^{-4}–10^{-3} μm. After the final stage, the average radius of droplets is 0.05–0.5 μm. Therefore, the Knudsen number (Kn) changes continuously from the free molecular flow region to the slip flow region [14]. The growth of large and small water droplets in supersaturated steam is described in Figure 1. The hollow circles represent water droplets, and the solid circles represent vapour molecules. Figure 1a shows the continuous flow model, and Figure 1b shows the free molecular flow model. According to the theory of gas dynamics, the collision frequency of vapour molecules to the nucleus of condensation is related to the average free path of the vapour molecules and the radius of the water droplets. The larger the Knudsen number, the smaller the diameter of the droplet. The equation for calculating Kn [15] is

$$Kn = \frac{3\mu\sqrt{RT_s}}{4pr}, \tag{1}$$

where μ is the steam dynamic viscosity, in Pa·s; T_s is the steam saturation temperature, in K; R is the steam gas constant; p is the steam pressure, in Pa; and r is the droplet radius, in m.

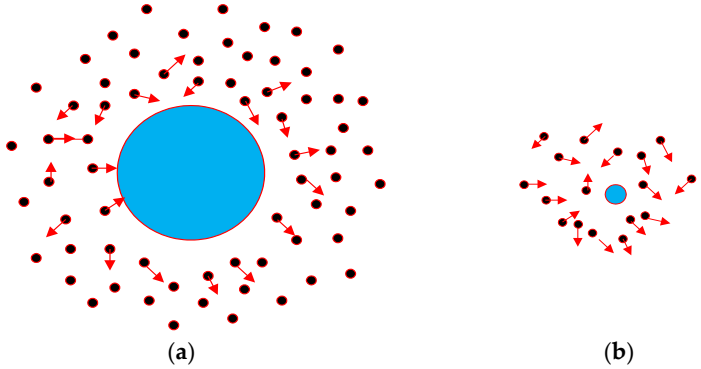

Figure 1. Growth of water droplets in supersaturated steam. (**a**) Knudsen number (Kn) < 0.01; and (**b**) Kn > 4.5.

When Kn < 0.01, the condensation flow of supersaturated steam belongs to the continuous flow region. When Kn > 4.5, the condensation flow of supersaturated steam belongs to free molecular flow. When $0.01 \leq Kn \leq 4.5$, the flow belongs to the transition region. The Kn decreases as the droplets grow. The relationship between Kn and the droplet diameter is given in Figure 2.

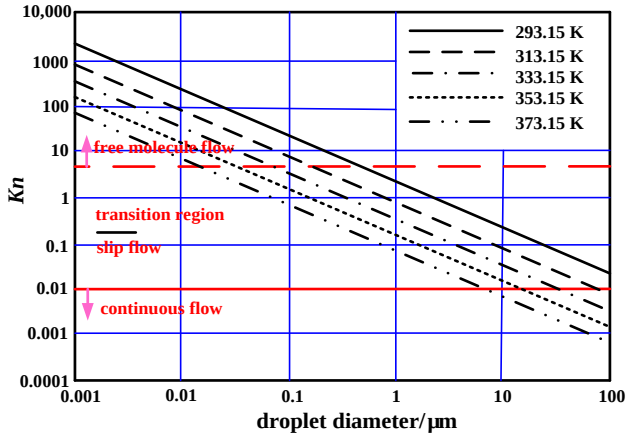

Figure 2. Relationship between the Kn and water droplet diameter.

Kn is an important parameter with respect to controlling heat and mass transfer. According to the different values of *Kn*, the combination of water droplets and the surrounding environment can be divided into three regions, as shown in Figure 3. The inner layer is the condensation nucleus, whose temperature can be regarded as evenly distributed. The middle layer is the Knudsen layer, and the heat and mass transfer in this layer are determined by molecular dynamics. The outer layer is the continuous flow region, where the heat and mass transfer are determined by the gas control equation under the assumption of a continuous medium. The process of water droplet growth will pass through the transition region.

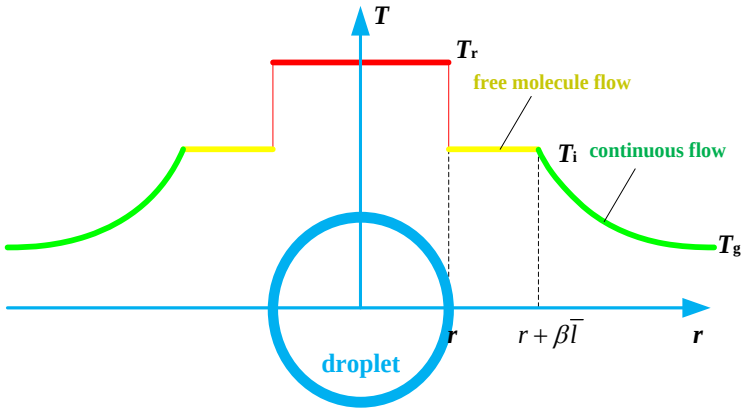

Figure 3. Temperature distribution of the droplets surrounding the environment in the Langmuir model.

At present, research on describing the droplet growth process of the transition region is lacking and a precise mathematical model does not exist. To describe the growth model of water droplets in the full-scale range, three methods are usually adopted. (1) The correction factor is multiplied with consideration to the influence of gas molecular dynamics before the continuous flow model or the free molecular flow model is applied. The correction factor is a function of *Kn* which is generally used to correct the heat transfer coefficient of the droplet surface and the surrounding steam, or the mass flow of the droplets and the surrounding steam [2,10]; (2) Modification is carried out via intermediate interpolation to the molecular dynamics model and the continuum dynamics model. The modified formula satisfies both sides of the limit condition. When the water droplet radius tends to the critical radius, the modified formula satisfies the molecular dynamics model. When the radius of the water droplet tends to infinity, the modified formula satisfies the kinetic model [12,13]; (3) A transition layer is assumed to exist between the water droplets and the surrounding steam. The energy flow equations between the water droplet surface, the imaginary interface, and the continuous steam are deduced. The two equations are used to eliminate the interface temperature term, and the water droplet growth model is then obtained [16].

The three aforementioned methods have shortcomings. The correction factor is used in Method 1 to correct the heat transfer or mass transfer; thus, the predicted water droplet growth rate in the free molecular flow region and in the transition region is smaller. In addition, no exact formula exists for determining the water droplet temperature. Method 2 does not describe the growth process of water droplets in the transition region. However, the water droplet growth model in the transition region is only interpolated from the numerical solution. This model only considers the mass exchange between the water droplets and the surrounding steam unilaterally. The condensation coefficient strongly influences this model; unfortunately, the values of the condensation coefficient vary widely [17]. Method 3 has advantages with respect to model integrity; however, the mass transfer equation is not considered. When the temperature of the droplet is determined, the coefficient of condensation is not equal to the coefficient of evaporation because of the non-equilibrium state. The coefficient of adjustment differs under different experimental conditions. In practical calculations,

a constant between 0 and 9 is usually used. This approach introduces errors in the calculation of the droplet temperature.

The steam condensation rate on the surface of water droplets is mainly related to the rate of latent heat diffusion to the surrounding steam. The heat transfer coefficient of the water droplet surface is as follows:

$$\alpha_r = \frac{\lambda_g}{\gamma} \cdot \frac{1}{1 + \frac{6.684}{Pr_g} \cdot \frac{\gamma}{1+\gamma} \cdot Kn}, \tag{2}$$

where λ_g is the thermal conductivity of steam, in W·(m·K)$^{-1}$; Pr_g is the Prandtl number; and γ is the ratio of the specific heat of steam.

The heat transfer of a single droplet to the surrounding steam in unit time is as follows:

$$\dot{Q} = \frac{dQ}{dt} = 4\pi r^2 \alpha_r (T_r - T_g), \tag{3}$$

where T_r is the droplet temperature, in K; and T_g is the steam temperature, in K.

The droplet growth rate can be expressed by the increments of the droplet radius per unit time. Because the droplets are at the nanometre level, the heat capacity itself can be ignored. Therefore, $\dot{Q}$ should also be equal to the product of latent heat of condensation and steam condensation per unit time:

$$\frac{dQ}{dt} = h_{fg} \cdot \frac{dm}{dt} = h_{fg} \cdot 4\pi r^2 \rho_l \frac{dr}{dt}, \tag{4}$$

where ρ_l is the liquid density, in kg/m^3; h_{fg} is the latent heat of condensation, in J/kg; m is the mass of a water molecule, in kg; and dm/dt is the steam condensation per unit time, in kg/s.

According to the flux matching between condensation nodules and transition layers, Gyarmathy used the Fick diffusivity and the Fourier thermal conductivity to calculate the growth rate of water droplets under the two limiting conditions of $Kn << 1$ and $Kn >> 1$. The Gyarmathy model of water droplet growth can be obtained as follows [6]:

$$\frac{dr}{dt} = \frac{\lambda_g}{\rho_l h_{fg}} \cdot \frac{1}{1 + \frac{6.684}{\mathrm{Pr}_g} \cdot \frac{\gamma}{1+\gamma} \cdot \frac{Kn}{\alpha_{th}}} \cdot \frac{T_r - T_g}{r}, \tag{5}$$

where α_{th} is the heat capacity of the vapour molecules' springback droplet surface, in J/(kg·K).

For condensation flow in the last stage of the steam turbine, let Pr_g = 1.2, γ = 1.3, and $T_r - T_g = \Delta T(1 - r^*/r)$. Substituting these quantities into Equation (5), we obtain

$$\frac{dr}{dt} = \frac{\lambda_g}{\rho_l h_{fg}} \cdot \frac{1 - r^*/r}{r(1 + 3.18Kn)} \cdot \Delta T, \tag{6}$$

where r^* is the critical droplet radius in m, and ΔT is the degree of super-cooling.

According to the flux matching between the continuous flow region layer and the Knudsen layer, the water droplet growth model under arbitrary Kn is studied on the basis of the Gyarmathy model and Langmuir's three-layer theoretical model of water droplets, and the model is modified at 10–30 kPa [8,9]. Young proposed β as the correction factor affecting the growth rate of water droplets in the Knudsen layer. The Young model is as follows:

$$\frac{dr}{dt} = \frac{\lambda_g}{\rho_l h_{fg} r} \cdot \frac{1 - r^*/r}{\frac{1}{1+2\beta Kn} + 3.78(1 - \xi) \cdot \frac{Kn}{\mathrm{Pr}_g}} \cdot \Delta T, \tag{7}$$

$$\xi = \frac{RT_s}{h_{fg}} \cdot [\psi(P) - 0.5 - \frac{2 - q_c}{2q_c} \cdot \frac{\gamma + 1}{2(\gamma - 1)} \cdot \frac{RT_s}{h_{fg}}], \tag{8}$$

$$\psi(P) = 3.25[1 - \tanh(\frac{p}{10^4} - 2)], \tag{9}$$

where ξ is a semi-empirical correction coefficient; $\Psi(P)$ is a correction factor of water droplet growth; and β is the correction factor.

2.2. Coupled Model of Heat and Mass Balance

Water droplet growth is mainly limited by two factors: the mass condensation rate on the droplet surface, and the rate at which condensation latent heat is transferred from the water droplet surface to the surrounding steam. Because of the high condensation latent heat of water, Chandler et al. proposed that the water droplet growth is mainly affected by the second factor [18]. Various water droplet growth models include uncertain factors, especially the value of the heat transfer temperature difference. We here propose a coupled model of heat and mass balance for droplet growth; this model is based on heat transfer equilibrium and mass transfer equilibrium. A saturated steam film is considered to exist between a droplet and the supersaturated steam around the droplet. The pressure and temperature of the saturated steam film can be determined. The droplet surface can be coupled by the heat transfer equation and the mass transfer equation. According to the Maxwell model, the mass transfer process on the droplet surface can be expressed as

$$\frac{dm}{dt} = 4\pi r^2 \rho_l \frac{dr}{dt} = 4\pi r^2 \zeta\left(\rho_g - \rho_s(T_r, r)\right) = 4\pi r^2 \zeta\left[\frac{p}{RT_g} - \frac{p_s(T_r, r)}{RT_r}\right]. \tag{10}$$

The saturation pressure of the droplet surface is

$$p_s(T_r, r) = p_s(T_r)\exp\left(\frac{2\sigma}{r\rho_l RT_r}\right). \tag{11}$$

The mass transfer coefficient can be obtained from the dimensionless Nusselt number for mass transfer (Nu_M):

$$\zeta = \frac{Nu_M D}{2r}, \tag{12}$$

where D is the self-diffusion coefficient of steam; and $p_s(T_r)$ is the saturation pressure corresponding to droplet temperature, in Pa.

In the continuous flow region, $Nu_M^{ct} = 2$. In the free molecular flow region, $Nu_M^{fm} = 0.7979\ \mu/\rho_g DKn$ [19]. The dimensionless mass transfer coefficient can be expressed as:

$$Nu_M = \frac{Nu_M^{ct} Nu_M^{fm}}{Nu_M^{ct} + Nu_M^{fm}}. \tag{13}$$

There are two directions for condensation latent heat generated by the water droplet growth process. One is the heat transfer to the surrounding steam through convection heat transfer; the other is the internal energy increment of the droplet itself. The heat transfer process between a droplet and steam can be expressed as:

$$h_{fg}\frac{dm}{dt} = 4\pi r^2 \alpha(T_r - T_g) + mC_p\frac{dT_r}{dt}, \tag{14}$$

where C_p is the constant-pressure specific heat, in J/(kg·K).

Because the diameter of a primary droplet is less than 100 nm, the magnitude of its internal energy change is substantially lower than the magnitude of the latent heat of condensation. Therefore, the second terms on the right side of Equation (14) can be neglected. The coupling model of heat and mass balance can be obtained by combining Equations (10) and (14):

$$\frac{dr}{dt} = \frac{\alpha}{\rho_l h_{fg}}(T_r - T_g). \tag{15}$$

The convective heat transfer coefficient of a droplet and the surrounding steam can be determined from the Nusselt number (Nu) [20]:

$$\alpha \equiv \frac{Nu \cdot \lambda_g}{2r} = \frac{\lambda_g}{r[1 + 3.78(1-\xi)K_n P_{rg}{}^{-1}]}. \tag{16}$$

The droplet temperature T_r can be determined by the following equation:

$$\frac{p}{RT_g} + \frac{\alpha}{\zeta}T_g = \frac{\alpha}{\zeta}T_r + \frac{p_s(T_r)}{RT_r}\exp\left(\frac{2\sigma}{r\rho_l RT_r}\right). \tag{17}$$

The droplet growth rate can be obtained by introducing T_r and α into Equation (15). The coupled model of heat and mass balance proposed in this paper is that given by Equation (15).

2.3. Droplet Surface Tension Correction

The liquid-plane surface tension equation [21] is:

$$\sigma_0 = 0.2358\left(1 - \frac{T_s}{647.3}\right)^{1.256}\left[1 - 0.625\left(1 - \frac{T_s}{647.3}\right)\right]. \tag{18}$$

According to the Gibbs surface tension theory, high error is introduced when the surface tension is calculated using the plane tension model. Three correction methods have been developed.

Tolman considered the capillary phenomenon at the bending interface and modified the plane surface tension model [22]:

$$\sigma = \frac{r\sigma_0}{r + 2\delta'}, \tag{19}$$

where σ_0 is the liquid plane surface tension and δ is the Tolman length.

On the basis of isothermal and isobaric condensation, Kashchiev corrected σ_0 in the ideal gas state as follows [23]:

$$\sigma = \sigma_0[1 - \exp(-\frac{r\Delta p_s}{2\sigma_0})]. \tag{20}$$

The Benson model is as follows [24]:

$$\sigma = \sigma_0 \cdot \left(1 - \frac{\sqrt[3]{\rho_l / m}}{4.836r}\right). \tag{21}$$

However, the two-phase condensation flow in a steam turbine is complicated and differs dramatically from the ideal gas parameter. Therefore, the Kashchiev model cannot be used. Huang used the Tolman model and the Benson model to calculate the condensation flow in a de Laval nozzle [21]. The Benson model most closely matches the experimental data; therefore, in the present paper, the Benson model is used to correct the plane surface tension equation.

3. Calculation Results and Analysis

3.1. Modelling Verification

On the basis of the experimental data of Peters and Meyers [25], the growth rate of water droplets was calculated using the three models under the conditions of p = 3.693 kPa and T_g = 284.4 K. The results are shown in Figure 4. Assuming that the condensation nucleus and vapour phase are in a metastable equilibrium state, r^* = 1.1 × 10^{-9} m. The radius of the water droplets increases gradually because of the continuous addition of vapour molecules. Condensation latent heat causes the droplet temperature T_r to change continuously and finally approach the vapour-phase equilibrium temperature T_g.

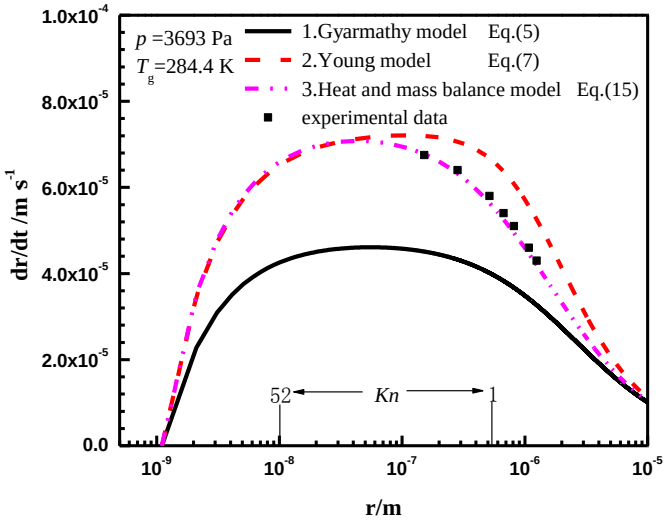

Figure 4. Comparison of the water droplet growth models.

Figure 4 shows that the value of Kn decreases with increasing droplet radius. The droplet growth rates calculated using Model 2 and Model 3 are substantially higher than that calculated using Model 1. The calculations using Model 2 and Model 3 show faster water droplet growth and greater release of latent heat in unit time. Thus, the condensation wave will be more obvious. In the free molecular flow region, the correction of the convective heat transfer coefficient of Model 1 and Model 3 can interfere with the influence of the droplet temperature difference on the droplet growth rate. Model 1 predicts a smaller droplet growth rate in the free molecular region and transition region because this model lacks an exact expression for the mass and energy transfer between the transition layer and the droplet surface. Model 1 only considers the influence of the gas molecular dynamics through the correction factor, which introduces a defect in physical consistency. When $Kn < 20$, the droplet growth rates predicted by Model 2 and Model 3 basically coincide. However, when $Kn = 20$, the two calculation results differ, with the maximum difference in the transition zone when $Kn \approx 1$. Dramatic differences are observed in the droplet growth rate calculation results in the transition region. When $Kn < 1$, the difference between the three models decreases. Notably, when $Kn < 0.1$, the three models coincide completely, which indicates that the three models are the same in the continuous flow.

Figure 5 shows the relationship between droplet temperature and radius. The droplet temperature of Model 1 is based on the following assumption: $T_r - T_g = \Delta T(1 - r^*/r)$. According to this equation, when $r >> r^*$, the heat transfer temperature difference is equal to the degree of supercooling, which is not in accordance with the actual situation because, when droplets grow into large drops, steam has been completely restored from the supersaturation state to thermodynamic equilibrium [26]. The temperature of the steam phase cannot be the supercooling temperature T_g. The temperature of vapour molecules in wet steam should be equal to the saturation temperature T_s. The droplets accept the latent heat of condensation and keep the surface temperature approximately equal to that of the surrounding steam via the heat transfer between the surface and vapour. Therefore, the droplet surface temperature T_r should be slightly larger than the steam saturated temperature T_s. As a result, the wet steam can remain in a dynamic equilibrium state.

The droplet temperature calculated by Model 3 agrees with that of Model 1 at the initial stage of nucleation. However, when the equilibrium state is restored, the calculated value of Model 3 is approximately 1 K higher than that of Model 1. The droplet temperature calculated by Model 2 clearly differs. The maximum difference is 15 K, which is not consistent with the actual situation. After condensation nuclei form, droplets rapidly grow and release latent heat to allow the gas–liquid two-phase flow to rapidly return to the equilibrium state. In the near-equilibrium state, the heat transfer between the droplet and the surrounding steam cannot be under a large temperature difference.

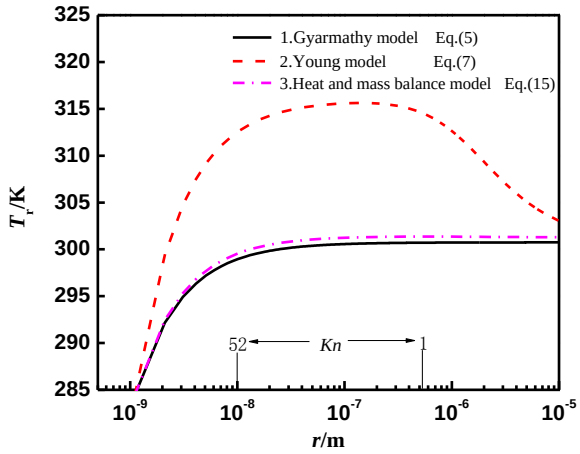

Figure 5. The relationship between the droplet temperature and the radius.

Through the aforementioned analysis, Model 3 can correctly calculate the droplet temperature; in addition, in the free molecular flow region, it coincides with Model 2, which is widely used at present. In the transition region, Model 3 is in good agreement with the experimental data of Peters and Meyers [25]. In the continuous region, Model 3 coincides with Model 1. The results reveal that the droplet growth in the transition region depends not only on the rate of the latent heat transferred from the droplet surface to the surrounding steam but also on the molecular dynamics of the vapour (which cannot be ignored). Therefore, Model 3, derived in this paper, can accurately predict the droplet growth rate in the full range of *Kn*.

3.2. Wet Steam Condensation Flow Analysis

To verify the reliability of the heat and mass balance model, we use the Benson model to modify the droplet surface tension. The nucleation rate is calculated by the Wölk–Strey experimental correction model [4,27]. The droplet growth rates are calculated by the Gyarmathy model, the Young model, and the heat and mass balance model. The non-equilibrium condensation flow of a de Laval nozzle is simulated; the nozzle profile is shown in Figure 6. The inlet diameter of the nozzle is 8 cm, the exit diameter is 4.746 cm, the throat is located at x = 0 cm, and the nozzle length is 23 cm. The inlet total pressure is P_0 = 80.2 kPa, and inlet total temperature is T_0 = 390.15 K. The exit is supersonic flow. The two-order TVD (Total Variation Diminishing) difference scheme and the time marching method are used to solve the problem [28]. In this paper, the flow field of a Laval nozzle is calculated under different grid numbers, such as 1.6×10^4, 3.2×10^4, 4.8×10^4, 6.4×10^4. When the grid number is higher than 3.2×10^4, the flow rate of the nozzle is near to steadiness. It is concluded that the 3.2×10^4 grids have grid independence, which can be used to solve the problem of a Laval nozzle.

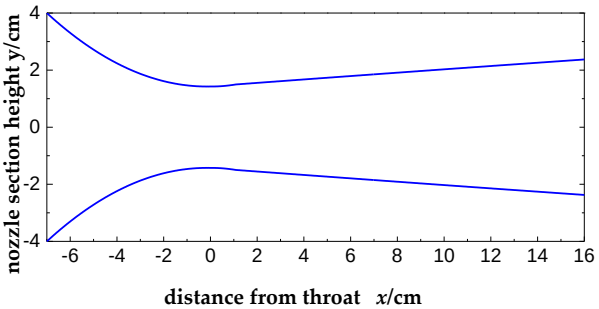

Figure 6. Geometric data of the de Laval nozzle.

The pressure distributions at the axis of the nozzle under the three droplet growth models are given in Figure 7. The *Kn* range of the droplet growth stage (from the nucleation start to the nozzle exit) in the nozzle condensation flow is 4.43–39.21. That is, the flow is in the transition region and the free molecular flow region. The nucleation rate and degree of supercooling distribution at the axis of the nozzle under the three droplet growth models are shown in Figure 8. The droplet number and radius distribution at the axis of the nozzle under the three droplet growth models are given in Figure 9.

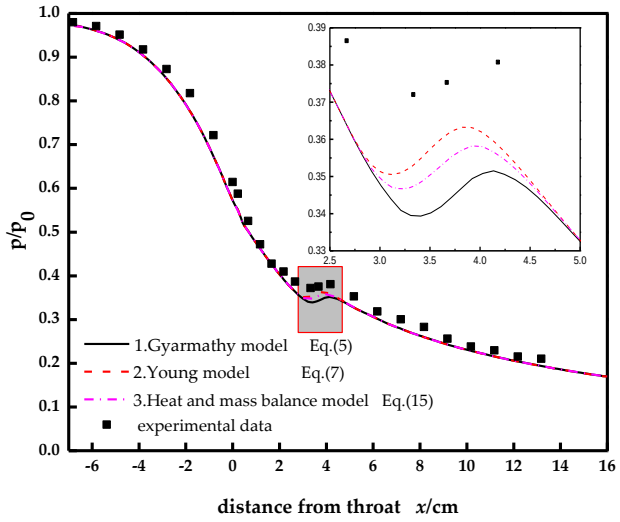

Figure 7. Pressure ratio along the nozzle axis compared with experimental data.

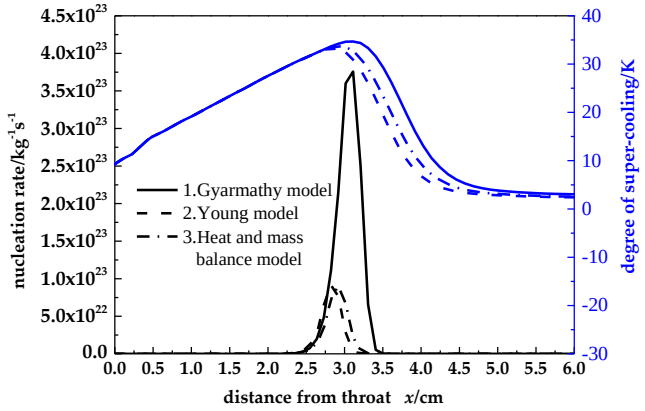

Figure 8. Degree of supercooling and nucleation rate distribution along the nozzle axis.

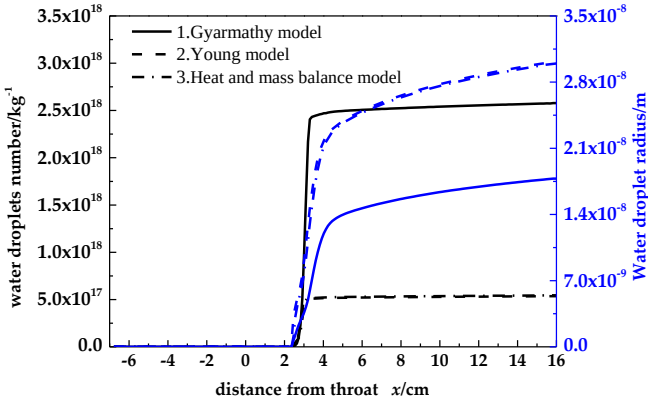

Figure 9. Droplet number and radius distribution along the nozzle axis.

In Figure 4, the droplet growth rate predicted by Model 1 is the smallest. The droplet radius distribution in Figure 9 confirms this characteristic; that is, the average radius of Model 1 is the smallest. At the nozzle exit, the droplet radius value predicted by Model 2 and Model 3 is 1.69 times greater than that predicted by Model 1. Droplets in Model 2 and Model 3 increase more rapidly over the same time period. More latent heat of condensation is released to the vapour phase, the pressure jump is more obvious, and the condensation occurs at a slight forward position. Figure 7 shows this characteristic. In addition, the release of latent heat leads to the increase in vapour-phase temperature and to the decrease in the degree of supercooling. As both Model 2 and Model 3 predict the production of more latent heat, the degree of supercooling is less than that predicted by Model 1 before reaching the equilibrium state, as shown in Figure 8. The degree of supercooling strongly affects the nucleation rate. Therefore, the nucleation rate value calculated by Model 2 and Model 3 is substantially smaller than that calculated by Model 1. Figure 8 shows that the nucleation rate is very sensitive to the degree of supercooling. When the degree of supercooling difference is approximately 1 K, the nucleation rate is 20% lower than that predicted by Model 1. With the decrease in the nucleation rate, the droplet number per unit mass decreases. The trend of the change in droplet number is similar to that of the change in the nucleation rate, and the droplet number predicted by Model 1 is approximately 5 times greater than those predicted by Model 2 and Model 3. The calculation results show that the pressure jump degrees calculated by the Young model and the heat and mass balance model are substantially greater than that calculated by the Gyarmathy model. The effects of different models on the nucleation rate, the droplet number, and the droplet radius are very obvious.

4. Conclusions

The study of the condensation flow of wet steam is important for improving the efficiency of steam turbines. On the basis of spontaneous condensation theory, the classical water droplet growth model was deduced and summarised. A coupled model of heat and mass balance was obtained. The droplet growth rate was calculated using the Gyarmathy model, the Young model, and the model deduced in this paper. The heat and mass balance model correctly calculated the droplet temperature. In the free molecular flow region, the developed model coincides with the Young model, which is widely used at present. In the transition region, the developed model is in good agreement with the experimental data of Peters and Meyer. In the continuous region, it coincides with the Gyarmathy model. The heat and mass balance model can be used to accurately describe droplet growth in the whole range of Kn. To reveal the influence of the droplet growth model on the condensation flow parameter, we used these models to calculate de Laval nozzle condensation flow. The influence of different droplet growth models on the condensation flow parameters was found to be very obvious.

Acknowledgments: The authors are thankful for the support provided by the Science and Technology Planning Project of Guangdong Province, China (Grant No. 2015B010101002), the National Science and Technology Support Program of China (Grant No. 2014BAA06B01) and the Fundamental Research Funds for the Central Universities of China (Grant No. 2016XS106).

Author Contributions: All authors contributed to this work. Xu Han is the main author of this work. Zhonghe Han guided the analysis and the writing of the paper. Wei Zeng and Zhi Wang assisted with the modeling. Jiangbo Qian provided suggestions with respect to article modification.

Conflicts of Interest: The authors declare no conflict of interest.

References

1. Hanak, D.P.; Kolios, A.J.; Biliyok, C.; Manovic, V. Probabilistic performance assessment of a coal-fired power plant. *Appl. Energy* **2015**, *141*, 350–364. [CrossRef]
2. Yousefi Rad, E.; Mahpeykar, M.R. A Novel Hybrid Approach for Numerical Modeling of the Nucleating Flow in Laval Nozzle and Transonic Steam Turbine Blades. *Energies* **2017**, *10*, 1285. [CrossRef]
3. Yang, Y.; Walther, J.H.; Yan, Y.; Wen, C. CFD modelling of condensation process of water vapor in supersonic flows. *Appl. Therm. Eng.* **2017**, *115*, 1357–1362. [CrossRef]

4. Han, Z.; Han, X.; Li, H.; Li, P. Comparative study of homogeneous nucleation rate models for wet steam condensing flows. *Korean J. Chem. Eng.* **2016**, *33*, 3487–3492. [CrossRef]
5. Han, Z.; Han, X.; Wang, Z. Numeric simulation of wet-steam two-phase condensing flow in a steam turbine cascade. *J. Braz. Soc. Mech. Sci. Eng.* **2017**, *39*, 1189–1199. [CrossRef]
6. Gyarmathy, G. The spherical droplet in gaseous carrier streams: Review and synthesis. *Multiph. Sci. Technol.* **1982**, *1*, 99–279. [CrossRef]
7. Hill, P.G. Condensation of water vapor during supersonic expansion in nozzles. *J. Fluid Mech.* **1966**, *25*, 593–620. [CrossRef]
8. White, A.J.; Young, J.B.; Walters, P.T. Experimental validation of condensing flow theory for a stationary cascade of steam turbine blades. *Philos. Trans. R. Soc. Lond.* **1996**, *354*, 59–88. [CrossRef]
9. Bakhtar, F.; Young, J.B.; White, A.J.; Simpson, D.A. Classical nucleation theory and its application to condensing steam flow calculations. *Proc. Inst. Mech. Eng. Part C J. Mech. Eng. Sci.* **2005**, *219*, 1315–1333. [CrossRef]
10. Heiler, M. *Instationäre Phänomene in Homogen/Heterogen Kondensierenden Düsen und Turbinenströmungen*; Universität Karlsruhe: Karlsruhe, Germany, 1999.
11. Delale, C.F.; Meier, G.E.A. A semi phenomenological droplet model of homogeneous nucleation from the vapor phase. *J. Chem. Phys.* **1993**, *98*, 9850–9858. [CrossRef]
12. Bakhtar, F.; Zamri, M. On the Performance of a Cascade of Improved Nozzle Blades in Nucleating Steam. *Proc. Inst. Mech. Eng. Part C J. Mech. Eng. Sci.* **2011**, *225*, 1649–1671. [CrossRef]
13. Bakhtar, F.; Mamat, Z.A.; Jadayel, O.C. On the performance of a cascade of improved turbine nozzle blades in nucleating steam. Part 2: Wake traverses. *Proc. Inst. Mech. Eng. Part C J. Mech. Eng. Sci.* **2009**, *223*, 1915–1929. [CrossRef]
14. Yang, Y.; Li, A.; Wen, C. Optimization of static vanes in a supersonic separator for gas purification. *Fuel Process. Technol.* **2016**, *156*, 265–270. [CrossRef]
15. Young, J.B. Two-dimensional, nonequilibrium, wet-steam calculation for nozzles and turbines cascade. *J. Turbomach.* **1992**, *114*, 567–579. [CrossRef]
16. Wen, C.; Yang, Y.; Walther, J.H.; Pang, K.M.; Feng, Y. Effects of delta wing on the particle flow in a novel gas supersonic separator. *Powder Technol.* **2016**, *304*, 261–267. [CrossRef]
17. Bakhtar, F.; Mashmoushy, H.; Jadayel, O.C. Calibration characteristics of a three-hole probe and a static tube in wet steam. *Int. J. Heat Fluid Flow* **2001**, *22*, 537–542. [CrossRef]
18. Chandler, K.; White, A.; Young, J. Non-equilibrium wet-steam calculations of unsteady low-pressure turbine flows. *Proc. Inst. Mech. Eng. Part A J. Power Energy* **2014**, *228*, 143–152. [CrossRef]
19. Luo, X.; Prast, B.; Dongen, M.V.; Hoeijmakers, H.W.M.; Yang, J. On phase transition in compressible flows: modelling and validation. *J. Fluid Mech.* **2006**, *548*, 403–430. [CrossRef]
20. Gerber, A.G. Two-phase eulerian/lagrangian model for nucleating steam flow. *J. Fluids Eng.* **2002**, *124*, 465–475. [CrossRef]
21. Xu, T.; Huang, Y. Development of experimental device for spontaneous condensation of supersaturated water vapor and determination of Wilson position of actual flow. *J. Xi'an Jiaotong Univ.* **1984**, *4*, 56–68.
22. Tolman, R.C. Consideration of the Gibbs theory of surface tension. *J. Chem. Phys.* **1948**, *16*, 758–774. [CrossRef]
23. Kashchiev, D. The kinetic approach to nucleation. *Cryst. Res. Technol.* **1984**, *19*, 1413–1423. [CrossRef]
24. Benson, G.C.; Shuttleworth, R. The surface energy of small nuclei. *J. Chem. Phys.* **1951**, *19*, 130–131. [CrossRef]
25. Peters, F.; Meyer, K.A.J. Measurement and interpretation of growth of mon dispersed water droplets suspended in pure vapour. *Int. J. Heat Mass Transf.* **1995**, *38*, 3285–3293. [CrossRef]
26. Yang, Y.; Wen, C. CFD modeling of particle behavior in supersonic flows with strong swirls for gas separation. *Sep. Purif. Technol.* **2017**, *174*, 22–28. [CrossRef]
27. Wölk, J.; Strey, R.; Heath, C.H.; Wyslouzil, B.E. Empirical function for homogeneous water nucleation rates. *J. Chem. Phys.* **2002**, *117*, 4954–4960. [CrossRef]
28. Han, X.; Han, Z.; Li, P. Influence of external particles on heterogeneous condensation flow in cascades. *Trans. Can. Soc. Mech. Eng.* **2017**, *41*, 265–280.